A Simple and Universal Technique To Extract One- and Two-Dimensional Nanomaterials from Contaminated Water

Bishnu Tiwari,[†] Dongyan Zhang,[†] Dustin Winslow,[†] Chee Huei Lee,[†,‡] Boyi Hao,[†] and Yoke Khin Yap[*,†]

[†]Department of Physics, Michigan Technological University, 1400 Townsend Drive, Houghton, Michigan 49931, United States

S *Supporting Information*

ABSTRACT: We demonstrate a universal approach to extract one- and two-dimensional nanomaterials from contaminated water, which is based on a microscopic oil−water interface trapping mechanism. Results indicate that carbon nanotubes, graphene, boron nitride nanotubes, boron nitride nanosheets, and zinc oxide nanowires can be successfully extracted from contaminated water at a successful rate of nearly 100%. The effects of surfactants, particle shape, and type of organic extraction fluids are evaluated. The proposed extraction mechanism is also supported by in situ monitoring of the extraction process. We believe that this extraction approach will prove important for the purification of water contaminated by nanoparticles and will support the widespread adoption of nanomaterial applications.

KEYWORDS: *water contamination, water purification, nanotubes, graphene, nanosheets, nanowires*
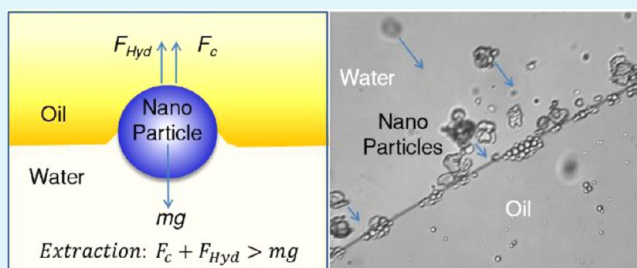
INTRODUCTION

The increasing interest in nanotechnology has promoted the use of nanomaterials in basic research and industrial applications.[1−3] In fact, nanomaterials are widely used in consumer products such as sunscreens, sports equipment, and many other products.[3] Unfortunately, the widespread adoption of nanomaterials has increased the possibility of releasing nanomaterials into the environment[4] during manufacture, delivery, and disposal of the products.[5,6] These nanoparticles, released to the environment, will eventually contaminate water and be ingested by human beings and other living creatures.

There has been minimal research focused on the adverse impact nanomaterials may have on the environment. The hazards and risks of engineered nanomaterials are a serious concern for environmental toxicologists, chemists, and social scientists.[6,7] Ideally for a new technology to be successfully implemented, it needs to be shown that the technology does not cause adverse effects to the environment.[8] Therefore, unless the potential risks of introducing nanomaterials into the environment are properly addressed, it will hinder the industrialization of products incorporating nanotechnology.[8] In fact, the Environmental Protection Agency (EPA) has started projects to assess the environmental risk of nanomaterials.[4,9] As nanomaterials find further market penetration, it is essential that approaches to manage the adverse effects of nanomaterials on the environment and human health be developed.[10] Therefore, a straightforward technique to separate nanomaterials from contaminated water, for example, will help in the proper disposal of nanomaterials, which will decrease the potential environmental and health hazards. Such a technique will be indispensable for further development and adoption of nanotechnology. Recently, we found that microscopic fluid interface dynamics could be utilized to extract and remove nanomaterials from the contaminated water.[11] Here, the details of this novel extraction technique are described. Results indicate that our approach can be used to effectively remove one-dimensional (1D) and two-dimensional (2D) nanomaterials with an efficiency of almost 100%.

MATERIALS AND METHODS

Nanomaterials without Functionalization. Five different nanomaterials are prepared in the laboratory for use in the extraction study. Multiwalled carbon nanotubes (MWCNTs),[12,13] boron nitride nanotubes (BNNTs),[14−16] and zinc oxide nanowires (ZnO NWs)[17] were synthesized by chemical vapor deposition. Multilayered graphene samples were prepared by expandable graphite powders (Grade 3772, > 98% carbon, Anthracite Industries, Inc., a subsidiary of Asbury Carbons, expansion ratio ∼1:300). The powders were heat shocked into multilayered graphene at 1000 °C in argon ambient. Multilayered boron nitride nanosheets (BNNs) were exfoliated by sonication (∼30 min) of BN powders (Grade AC6004, Momentive Performance Materials) in water.

Nanomaterials with Functionalization. MWCNTs, BNNTs, graphene, BNNs, and ZnO NWs were functionalized separately in two different surfactants: (1) 10 mg/mL of sodium cholate (Product # A17074, 99%, Alfa Aeser) and (2) 200 μM of methoxy-poly(ethylene glycol)-1,2-distearoylsn-glycero-3-phosphoethanolamine-N conjugates, which has an average molecular weight of 5000 (Product # mPEG-DSPE-5000−1GR; concentration, 200 μM; Laysan Bio, Inc.).[18] Both sodium cholate and mPEG-DSPE are water-soluble surfactants and different from those we reported for organic solvents.[19] Furthermore, to understand the effect of surfactant concentration on nanomaterial

extraction, the experiments were repeated by functionalization of MWCNTs with sodium cholate (10 mg/mL) and then decreasing the concentration of the sodium cholate surfactant in the suspension while keeping the amount of MWCNTs in the suspension constant. To decrease the concentration of surfactant in the suspension, the suspension was centrifuged at 8000 rpm for 1.5 h to condense the MWCNTs. After this, 2 mL of the supernatant was removed without extracting the condensed MWCNTs at the bottom of the vial. To preserve the total volume of suspension, 2 mL of distilled water was added to the solution, and the solution was hand shaken to ensure a uniform suspension. This produced a solution of sodium cholate concentration of 5 mg/mL. The process was repeated to produce a solution of 2.5 mg/mL sodium cholate in distilled water. This process of reduction of surfactant concentration in MWCNTs suspension was done by this repeated centrifugation method.

Geometry Effect of Nanomaterials. To understand the effect that the geometry of the particles has on the extraction efficacy, similar experiments were performed with nanospheres of different materials. Silica sphere (Catalog No. SIO2P020−01−100grams; particle size, 0.20 μm; Fiber Optic Center Inc.) and polystyrene nanosphere (Catalog # 100131−10, Product ID = C-PS-0.2, particle size =200 nm, Microspheres-Nanospheres) were used for investigating the effect of spherical shape of nanomaterials in extraction processing.

Extraction of Nanomaterials. Preparation of the contaminated water samples is described as follows. First, 1 mg of each nanomaterial was separately suspended in 4 mL of distilled water without surfactants. A sample of 0.1 mL of each suspension was coated and dried on silicon substrates for inspection. Then, 4 mL of semisynthetic hydrocarbon oil (KJLSS19 Premium Semi-Synthetic Vacuum Oil, Kurt J. Lesker) was added into each of the suspensions. The mixtures were hand shaken for 1 min to form an oil−water emulsion. The emulsion was then allowed to separate into oil and water phases at room temperature. After 1 day, the separated oil phase is removed by a pipet. A sample of 0.1 mL of the water phase after extraction was carefully transferred by a clean pipet and coated on a silicon substrate and dried on a hot plate. All coated samples were analyzed under a field emission scanning electron microscope (FESEM, Hitachi-S4700) and Raman spectroscopy (HORIBA, HR 800). Extraction of BNNSs was also performed with toluene (Sigma-Aldrich, ≥ 99.5%, ACS reagent) and hexane (Sigma-Aldrich, ≥ 98.5%, ACS reagent) by the same procedure.

Real-Time Detection of BNNS Extraction. A mixture of water, oil, and BNNSs was prepared as described earlier. Then 100 μL of the mixture was immediately placed on a glass slide under an inverted optical microscope (AmScope, IN480T-FL-3MT) for optical image capture.

RESULTS AND DISCUSSION

Extraction of Nonfunctionalized Nanomaterials from Water. In the first experiment, five types of 1D or 2D nanomaterials (1 mg each) were suspended in 4 mL of distilled water in separated glass vials by sonication. The preparation of all materials generally follows the methodology discussed in the Materials and Methods section. However, there were slight variations in preparation due to the nature of each material. The ZnO NWs were extracted by sonicating the sample in water for 5 min to avoid damage. The rest of the nanomaterials were extracted by sonicating the sample for 15 min to form a suspension. Figure 1 shows images of these samples at different steps of the extraction process. From left to right, the vials in each image are (1) multiwalled CNTs (MWCNT) in water, (2) graphene in water, (3) BNNTs in water, (4) water (reference), (5) BNNSs in water, and (6) ZnO NWs in water. As shown in Figure 1, panel a, the MWCNT and graphene suspension appear blackish in color, while those for BNNTs, BNNSs, and ZnO NWs are a whitish color. Oil is then gently added to every nanomaterial suspension and appears as a clear fluidic layer as
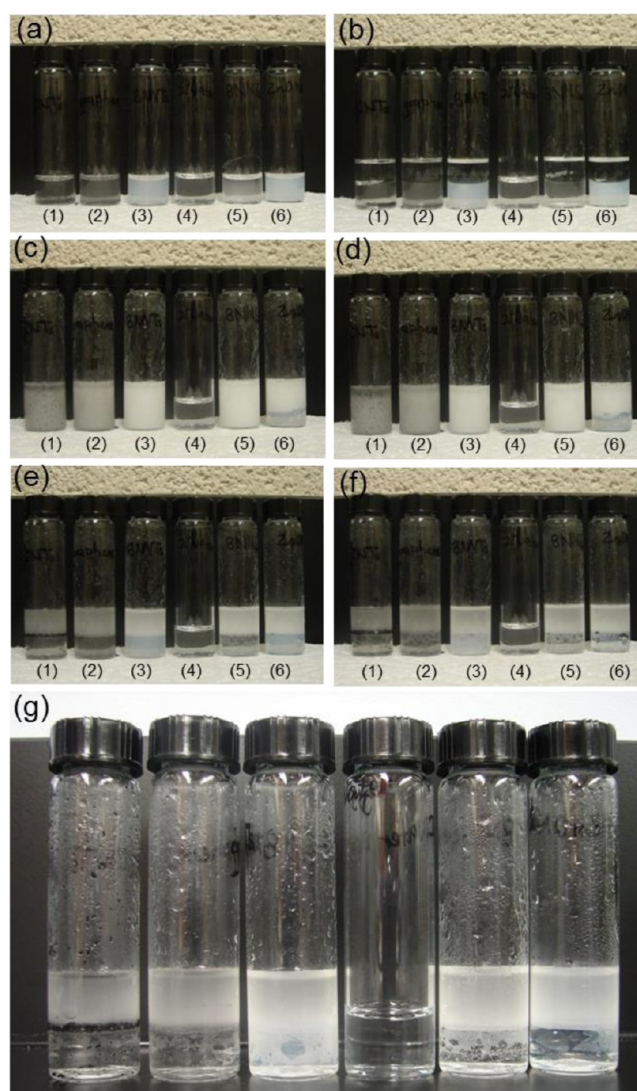

Figure 1. From left to right, bottles in each picture are (1) MWCNTs in water, (2) graphene in water, (3) BNNTs in water, (4) water, (5) BNNSs in water, and (6) ZnO NWs in water. (a) As suspended samples, (b) after adding oil on top, (c) after forming emulsion by hand shaking, (d) 2 min after emulsification, (e) 2 h after emulsification, (f) 1 day after emulsification, and (g) zoomed in view 1 day after emulsification.

shown in Figure 1, panel b. These two fluidic layers were then mixed into an emulsion by rigorous hand shaking. The vials are shown after being hand shaken for 1 min in Figure 1, panel c. The appearances of these suspensions (d) 2 min, (e) 2 h, and (f) 1 day after the emulsification are as shown. The separation of the emulsion occurs within 2 h, at which point the oil and water layers are clearly separated.

From the zoomed-in view (Figure 1g), nanomaterials have obviously been extracted out of the water phase and can be seen as dark or white condensates at the bottom of the oil phase. It should be noted that the inner glass walls have become coated with oil, which includes the glass wall at the bottom of the vials that surrounds the water phase. Therefore, some of the nanomaterials that are trapped in the oil phase stain the wall, which leads to the whitish and grayish coatings on the glass wall surrounding the water phase. Although, as will be shown, the water phase of each vial is now uncontaminated by the respective nanomaterials.

Extraction of nanomaterials from the contaminated water was confirmed by field emission scanning electron microscopy (FESEM) and Raman inspection. FESEM and Raman spectroscopy samples were prepared by drying 0.1 mL of the water phase samples on silicon substrates before and after the oil extraction process. As shown in Figure 2 (left column), clumps
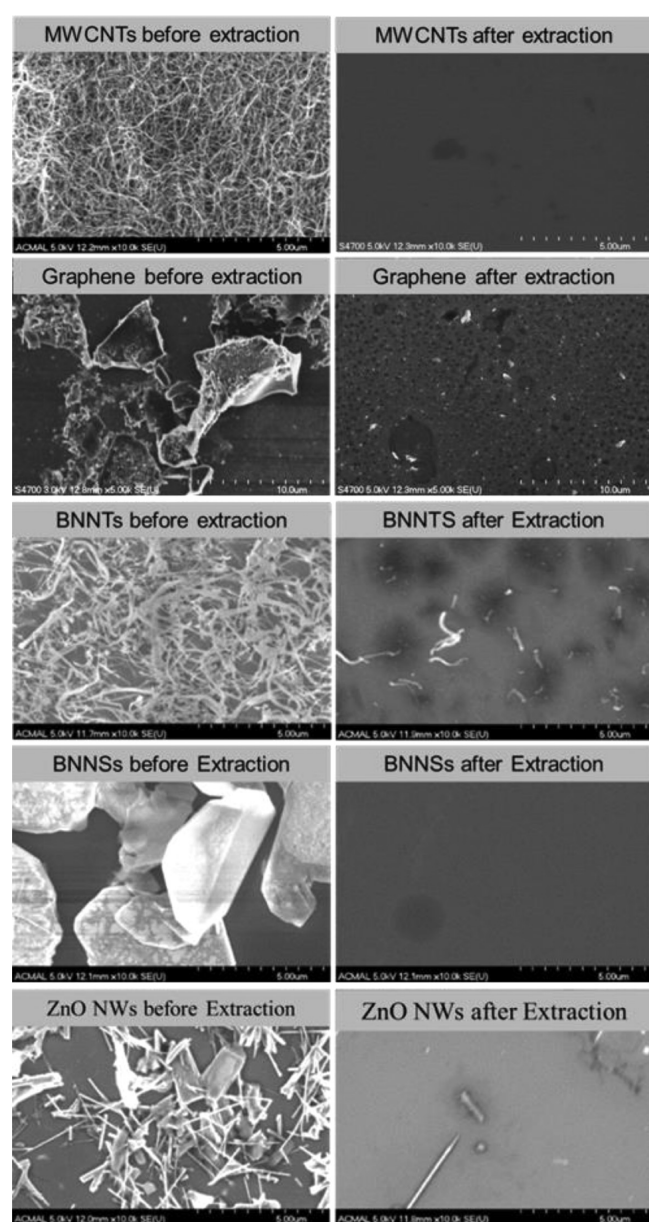

Figure 2. Images of coatings from the water phase of the nanomaterial suspension before (left column) and after (right column) extraction.

Each of these water samples has been characterized by Raman spectroscopy. The characteristic Raman peaks for MWCNTs, graphene, BNNTs, BNNSs, and ZnO NWs are detected for the pre extraction samples and shown in Figure 3,
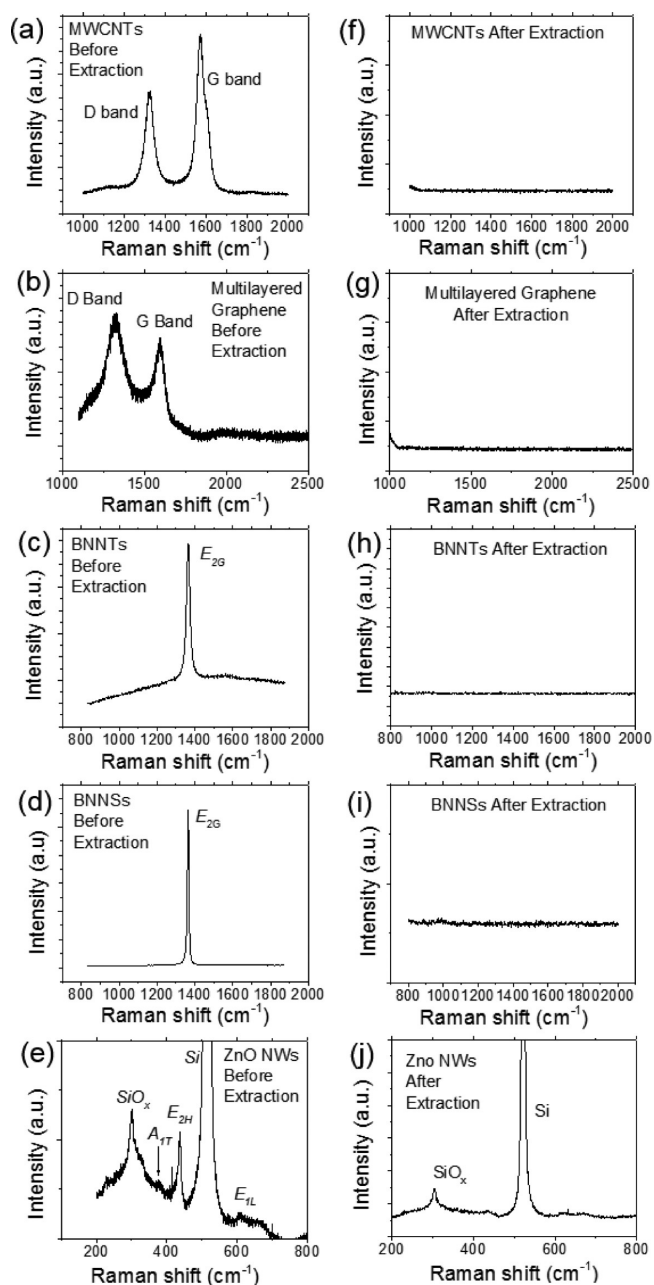

Figure 3. Raman spectra of (a) MWCNTs, (b) graphene, (c) BNNTs, (d) BNNSs, and (e) ZnO NWs sampled from water before extraction. Raman spectra after extraction are shown underneath (f, g, h, i, j) of each respective case.

of nanomaterials can be seen from the water-coated samples before the extraction process. However, nanomaterials are not found in the water phase after the extraction (right column). There are a few trace BNNTs and ZnO NWs detected in one or two locations of the water sample as shown, but otherwise no nanomaterials are detected from the water samples after extraction. A small amount oil can also be observed in these images. This result suggests successful purification of the water phase from contamination by these 1D and 2D nanomaterials. The extraction rate of the nanomaterials is nearly 100%.

panels a, b, c, d, and e, respectively. The Raman spectra after extraction for MWCNTs, graphene, BNNTs, BNNSs, and ZnO NWs are shown in Figure 3, panels f, g, h, i, and j, respectively. As shown, all the characteristic Raman peaks for the nanomaterials are not detected after the extraction process. This signifies that full purification of the water phase from the nanomaterial contaminants has been achieved. All of these Raman data are consistent with the FESEM images shown in Figure 2.
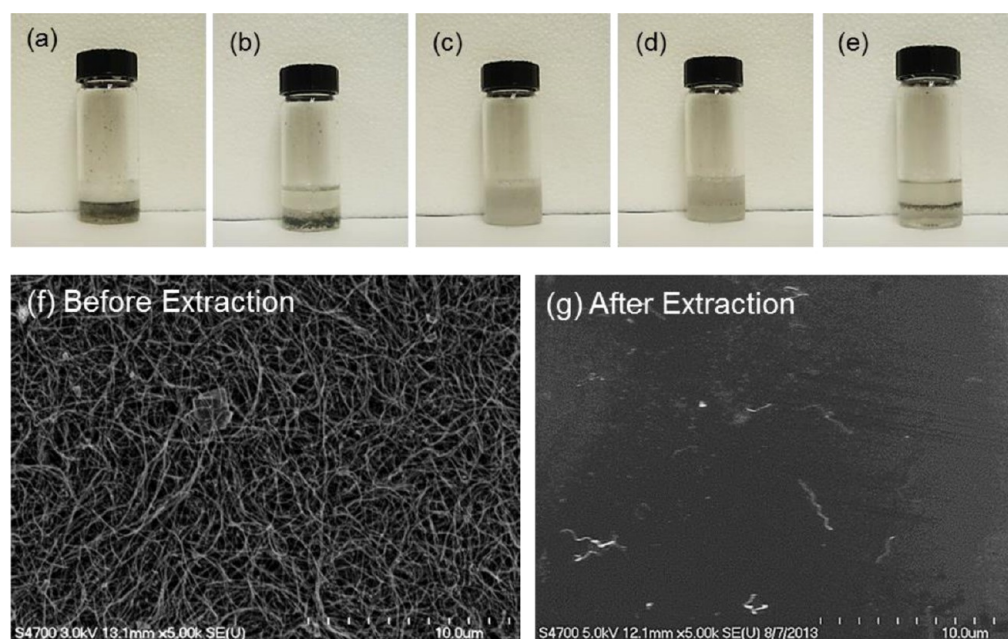
Figure 4. (a) As prepared MWCNT suspension in 2.5 mg/mL sodium cholate solution, (b) after adding oil, (c) after emulsification by hand shaking, (d) 2 min after emulsification, and (e) 1 day after separation. FESEM images of MWCNTs sampled from the 2.5 mg/mL of sodium cholate solution (f) before and (g) after extraction.
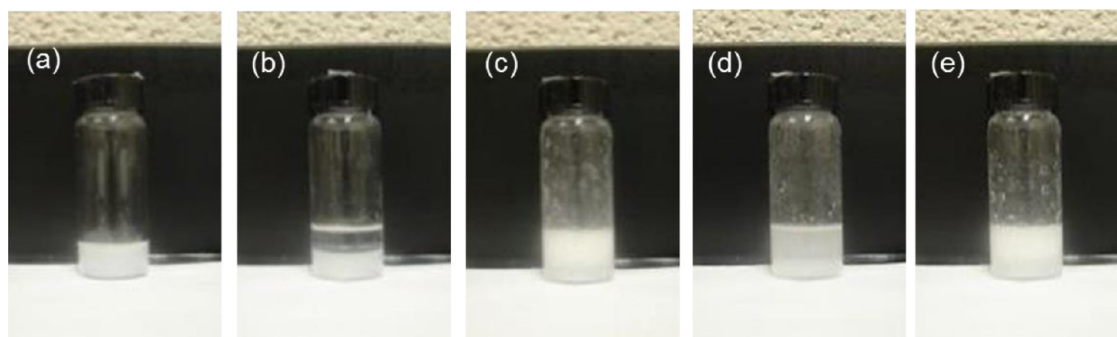

Figure 5. Images of (a) as prepared silica nanospheres suspension (b) after adding oil on top, (c) after emulsification by hand shaking, (d) 2 min after emulsification, and (e) 1 day after emulsification.

Extraction of Nanomaterials Functionalized with Surfactants. Next, the effect of an inorganic surfactant on the extraction of nanomaterials from water is examined. In place of distilled water, a sodium cholate ($NaClO_3$) solution with a concentration of 10 mg/mL was used for the experiments. Each sample was prepared by adding 1 mg of nanomaterial to the 4 mL of sodium cholate solution. Experiments were then repeated by adding oil on the suspensions and emulsification by hand shaking. Figure S1 (Supporting Information) shows photographs of the suspensions at each extraction step. As shown, the initially blackish or whitish suspension remained at the bottom of the vials after the separation step. The oil layers on top are hazed with some dark and white stains on the inner walls of the glass vials. These observations signify that the majority, if not all of the nanomaterials, were not extracted to the oil phase. To verify this, the oil phase was removed, and 0.1 mL of the water was extracted from each of the vials for FESEM inspection. As shown in Figure S2, nanomaterials are present in the water phase after the extraction process.

The effect of an organic surfactant was then examined. In this case, 1 mg of each type of nanomaterial was functionalized with methoxy-poly(ethylene glycol)-1, 2-distearoyl-sn-glycero-3-phosphoethanolamine-N conjugates (mPEG-DSPE, 200 μM). After the suspensions were prepared, the same extraction process was performed. Figure S3 shows the images of the suspensions at each step in the extraction process, and Figure S4 shows the FESEM images of water samples after the extraction. As shown in Figure S3, nanomaterials are present in the water phase without being extracted. This is proven from the FESEM images in Figure S4.

A series of experiments was then performed using MWCNTs to understand the effect of surfactant concentration on the extraction efficiency. For this case, sodium cholate at various concentrations was used. Results indicate that at a sodium cholate concentration of 2.5 mg/mL of suspended MWCNTs inside the sodium cholate solution can be extracted as shown in Figure 4. The initially dark colored suspension (a) became clear after the extraction process (e). FESEM images show that almost all of the MWCNTs (f) can be removed from the suspension and leave only a few trace MWCNTs in the water phase (g). Therefore, extraction is still possible for functionalized 1D nanomaterials at a sodium cholate concentration of 2.5 mg/mL ($\sim$5.8 mM).
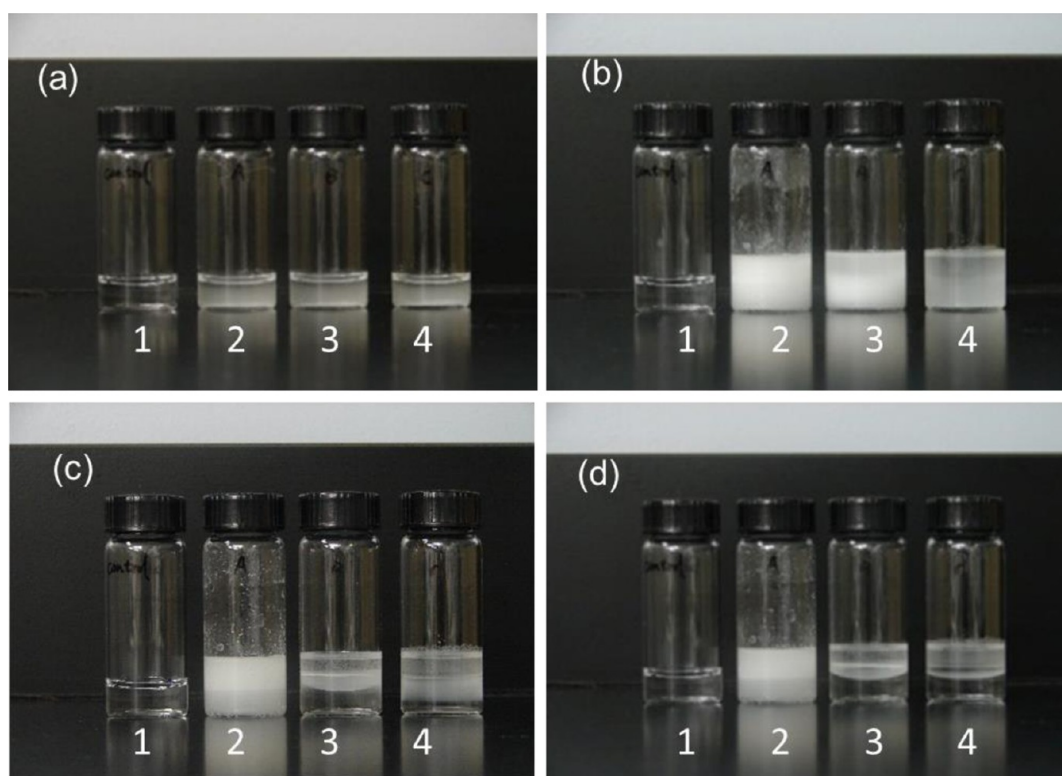
Figure 6. (a) As-prepared sample with distilled water (1) and three suspensions of BNNSs (2, 3, 4). (b) Samples after adding oil, toluene, and hexane to vials 2, 3, and 4, respectively. Samples (c) 2 h and (d) 1 day after emulsification by hand shaking.

This result is likely due to the reduction of water surface tension in the sodium cholate solution (as in other surfactants[20]). At excessive concentrations of sodium cholate, the surface tension of water and the capillary force generated at the oil−water interface will decrease. Trapping of nanomaterials at the oil−water interface will not happen when the capillary force cannot overcome the weight of the particles. The same explanation applies when mPEG-DSPE was used because the surfactant decreases the surface tension of the water resulting in a smaller capillary force acting on the MWCNTs. This will be further discussed in the extraction model later.

Effect of the Nanoparticle Shape. As has been shown, the aforementioned technique can effectively remove 1D and 2D nanomaterials from contaminated water. To verify the effect of particle shape on the extraction mechanism, extraction of zero-dimensional (0D) nanomaterials (spherical nanoparticles) was studied. The first round of experiments was performed on silica nanospheres (particle size 200 nm) by adding 1 mg of nanospheres to 4 mL of distilled water. The solution was sonicated for 30 min to ensure that the nanoparticles were evenly dispersed in the suspension. Figure 5 shows the images of the liquids at different phases of the extraction process. As shown, the water phase still remained milky after extraction, which suggests that the silica nanospheres remained in the water phase. This is proven by FESEM imaging of water samples before and after processing as shown in Figure S5. Similar experiments were repeated by using up to 16 mL of oil (four-times that of the volume of the suspension). However, these silica spheres could still not be extracted from the water phase. Therefore, it can be concluded that silica nanospheres cannot be extracted by the oil−water emulsion extraction method. The inability to extract the silica nanospheres may be because of the weight of the nanosphere, or it may be related to

shape of the particle. It may also be due to the viscosity of the oil used for forming the particle emulsion.

To further understand the effect of a nanomaterials weight on the extraction mechanism, the experiment was repeated using polystyrene nanospheres of the same diameter (200 nm), which have a lighter weight (~2.65 time lower in density). In addition, two different nonorganic solvents, toluene and hexane (less density than that of semisynthetic hydrocarbon oil), were used in the same set of experiments to explore whether the density of the solvent has any effect. In this experiment, three suspensions of polystyrene nanospheres (1 mg in 4 mL of distilled water in each) were prepared. Then 4 mL of semisynthetic hydrocarbon oil, toluene, and hexane were added to each suspension, respectively, to create three different extraction samples. The emulsion was then formed by hand shaking, and it was allowed to self-separate. Figure S6 shows the images of all these samples at different phases of processing. As shown, the water phase remained milky indicating the presence of nanospheres after extraction, which was confirmed by FESEM imaging (not shown here). The polystyrene nanospheres could not be extracted from the water phase in any of these cases. It is noted that toluene and hexane can be phase separated from the water phase effectively, and they appeared as clear layers on the water phase (Figure S6d). The above experiments indicate that the extractability of the materials is related to the shape of the particle and not simply their weights.

Comparing the Extraction with Various Types of Organic Fluids. To understand how the viscosity of the solvent used for forming the emulsion affects the extraction efficiency, additional experiments were performed by preparing BNNSs suspensions (2D instead of 0D) and attempting extraction with oil, toluene, and hexane. Figure 6 shows digital pictures at different phases of the extraction. As shown in
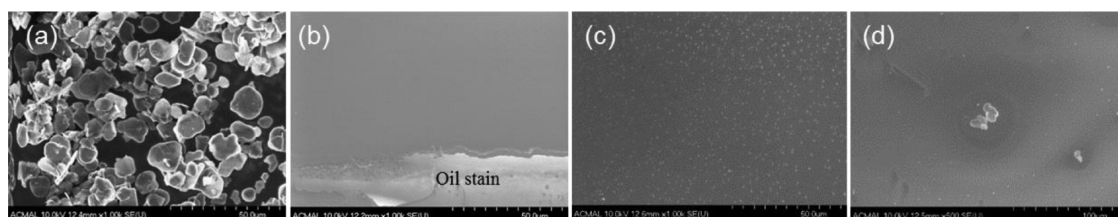
Figure 7. FESEM images of coatings sampled from the aqueous phase before extraction (a), and after extraction by (b) oil, (c) toluene, and (d) hexane.
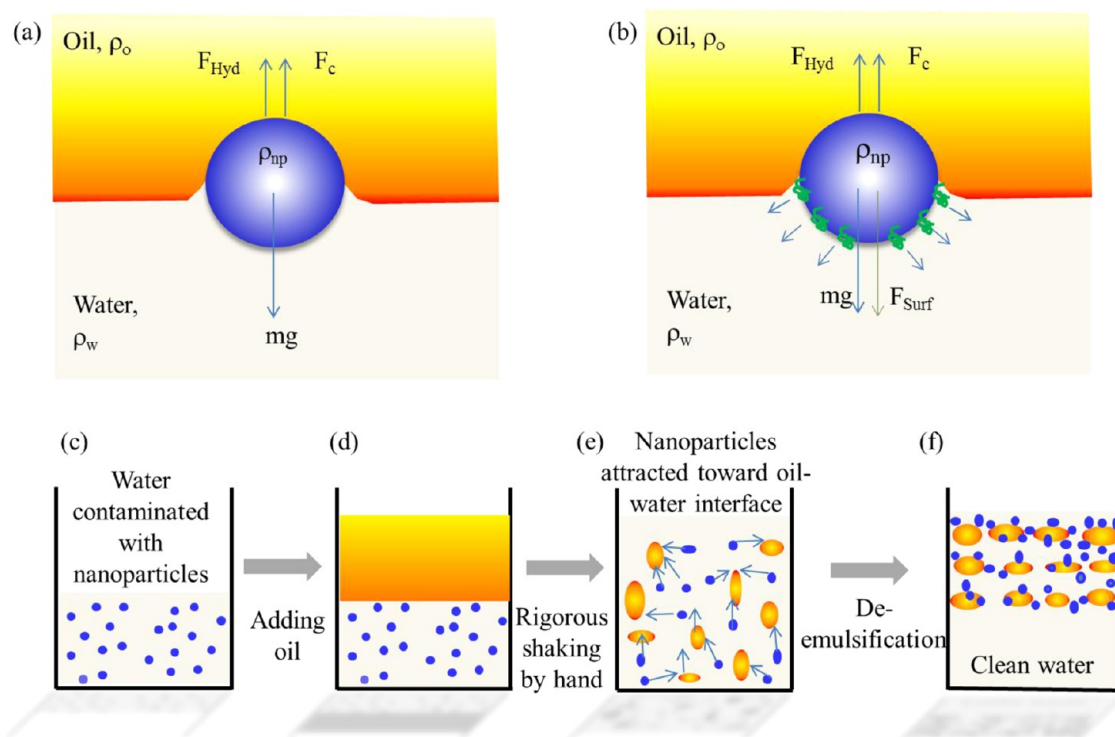

Figure 8. Force diagram of an (a) unfunctionalized and a (b) functionalized spherical nanoparticle. The schematic of the extraction mechanism are shown in panels c, d, e, and f. Please read the main text for detailed description.

Figure 6, panels c and d, the water phase after extraction with toluene and hexane has become clear only 2 h after emulsification. The water phase after extraction with oil remains milky due to the staining of oil on the inner glass wall. The toluene and hexane vials show no staining of the glass vials during the extraction processes.

From FESEM images in Figure 7, it can be seen that the BNNSs were extracted from the water phase by using oil, toluene, and hexane with almost 100% efficiency except one spot shown in Figure 7, panel d. As shown in Figure 7, panel b, the water sampled from the oil extraction case is stained with some residual oil as indicated by the charging white coatings at the bottom of the FESEM image. In contrast, the water phase was free from contamination by the organic fluids when toluene and hexane were used, as shown in Figure 7, panels c and d. This is another advantage to the use of toluene or hexane instead of oil. FESEM images were also taken from the toluene and hexane phases after extraction. As shown in Figure S7, BNNSs were extracted and trapped to the toluene and hexane phases after processing (sample from the oil phase cannot be taken due to charging from oil). The viscosities of water, oil, toluene, and hexane are ~0.89 mPas, ~102 mPas, ~0.59 mPas, and ~0.294 mPas, respectively. Their densities are ~1000 kg

m^{-3}, ~900 kg m^{-3}, ~866.9 kg m^{-3}, and ~654.8 kg m^{-3}, respectively. Therefore, there is no apparent trend relating the extraction efficiency to the densities and viscosities of the organic fluids used. On the other hand, the low viscosity and low density of toluene and hexane are responsible for the quick (within 2 h) liquid separation.

The Extraction Mechanism: A Particle at a Horizontal Oil–Water Interface. The extraction mechanism involved in the purification of water contaminated by nanomaterials is described as follows. The mechanism is formulated by referring to the interaction of macroparticles with macroscopic liquid interfaces.[21] Cavallaro et al. has shown that the curvature gradient produced by the particle at the macroscopic fluid interface attracts other particles to the region of high curvature and that this mechanism can be modeled as an electric field.[22] Consider a spherical nanoparticle with density ρ_{np} in an oil–water interface with densities of the organic fluid and water, ρ_o and ρ_w, respectively, where $\rho_{np} > \rho_w > \rho_o$. As shown in Figure 8, panel a, there are three different forces acting on the particle; the vertical capillary force (F_c) acting in the upward direction, which arises from the deformation of the fluid interface by the particle, the weight of the particle (mg), and the vertical component of the hydrostatic pressure force acting on the
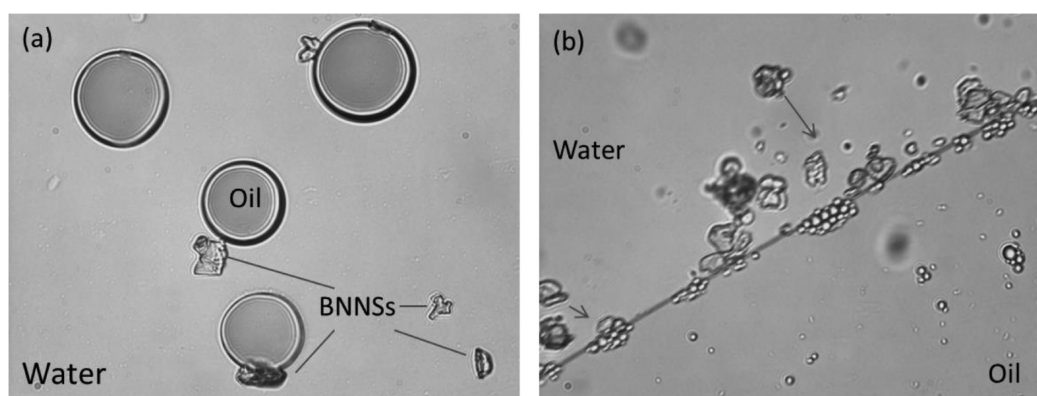
Figure 9. Optical images of (a) trapping of BNNSs at the boundary of oil droplets suspended in water. (b) Sweeping of oil droplets and BNNSs toward the oil−water interface.

particle (F_{Hyd}), which is acting upward. In the equilibrium condition, the relationship between three forces[23] is $F_c + F_{Hyd} =$ mg. Here, F_c depends solely on the nature of the interface deformation, which is dependent on the size and shape of the trapped particles.[22] Therefore, in addition to the mass of a particle, the size and shape of the particles are also equally important in bringing the particle to a stable equilibrium condition at the fluid interface. A similar force diagram for a surfactant functionalized spherical nanoparticle is shown in Figure 8, panel b. Here, the surfactant molecules introduce an additional hydrophilic force between the nanoparticle and the surrounding water, with a net downward F_{surf} as shown. In this case, $F_c + F_{Hyd} =$ mg + F_{surf}. We will discuss the case of functionalized particles later.

The schematic of the extraction process for unfunctionalized nanoparticles is illustrated in Figure 8, panels c, d, e, and f. During the formation of the emulsion, the nanomaterials come into contact with and are trapped at the oil−water interface between the small oil droplets and water within the emulsion, as shown in Figure 8, panel e. The nanoparticles first deform the interface and give rise to F_c between particles at the interface. As the oil and water separates, the nanomaterials trapped at the oil−water interface of the oil droplets are swept upward during phase separation (de-emulsification), as shown in Figure 8, panel f. Once the oil and water are completely separated, the nanomaterials are now contained within the oil phase. If the weight of the nanoparticles can overcome F_{Hyd}, the nanoparticles will condense at the bottom of the oil phase. However, if $F_{Hyd} \geq$ mg, the nanoparticles will remain stable in the oil phase for a long period of time unless a disturbance in the system is created.

In situ experiments were performed to verify the trapping of BNNSs by the oil−water interface. In this case, one drop (100 μL) of emulsion (oil-BNNS suspension) was placed on a glass plate under the optical focus of an inverted optical microscope. Optical pictures were then taken by use of a digital camera attached on the optical column. As shown in Figure 9, panel a, the BNNSs are trapped at the oil−water interface of oil droplets that are suspended in the water phase. These oil droplets and BNNSs quickly move toward the oil−water interface during the de-emulsification process, as shown in Figure 9, panel b. It is interesting to see that some BNNSs are also moving toward the oil−water interface of the separated fluids, presumably due to the capillary force generated by the distorter interfaces as the oil droplets and BNNSs merge into the oil phase.

For the case of functionalized nanomaterials (Figure 8b), the surfactant molecules are interfaced between the materials and the surrounding water. Here, the hydrophilic forces between the surfactant and water molecules, F_{surf}, are responsible for dispersing the nanomaterials in the water phase.[24] Since $F_c + F_{Hyd} =$ mg + F_{surf}, a stronger F_{surf} will tend to balance out the upward trapping force ($F_c + F_{Hyd}$). F_{surf} is larger when the concentration of the surfactant is higher as more surfactant molecules are adsorbed onto the nanomaterials so that they are more readily attracted to the water molecules. In this case, $F_c + F_{Hyd}$ may be overcome by mg + F_{surf}. Therefore, trapping of the nanoparticle at the oil−water interface will not happen. In addition, the surfactants will decrease the surface tension of water and hence decrease F_c on the particle. All these explain the failure of nanomaterial extraction when a high surfactant concentration is applied. Our results show that this issue can be resolved by diluting the concentration of surfactants prior to nanomaterial extraction.

The extraction mechanism can also explain why 1D and 2D materials are easier to extract than spherical nanoparticles. For the case of microparticles, it is known that the surface roughness and chemical heterogeneity will have an effect on the interface deformation produced by the particles through a quadrupole interaction.[25] This quadrupole interaction gives rise to the capillary interactions between the particles trapped at the fluid interface.[26] It has been shown that the deformation of the oil−water interface is higher if the shape of the particle trapped at the liquid interface is nonspherical, that is, ellipsoidal or polyhedral, or if the particles have surface roughness.[27] However, spherical microparticles with surface irregularities can produce undulating contact lines and deform the fluid interface. This interface deformation will give rise to capillary forces between such rough spherical particles.[28]

Experimentally, it was shown here that the extraction attempt of the spherical nanoparticles was not successful. Therefore, the nanospheres that were used were likely too smooth, too small, and were unable to sufficiently deform the fluid interface. This inability to adequately deform the interface meant that there was insufficient or no capillary force to trap the nanoparticles at the interface as the oil and water phases separated. The nanospheres were therefore unable to remain at the interface.

Another way to understand the failure to extract the spherical nanoparticles is in terms of the energy. The capillary energy is the product of the surface tension and the area of deformation,[21] and because the area of deformation is smaller for spherical particles than for 1D and 2D nanomaterials, they

are less likely to be trapped. Because of the same reason, a cylindrical rod will be attracted and rotated by the capillary force such that the surface along the length of the rod will preferentially come into contact with the interface.[25] Since the interface deformation is quadrupolar, a long-range capillary force arises between the particles, and this capillarity drives the particles along the interface curvature gradient along the path to where the total interfacial energy is at a minimum.[25] All the nanotubes, nanowires, and nanosheets used for our investigation were anisotropic in shape. Their anisotropic nature produces a quadrupolar deformation, which gives rise to larger capillary forces. These resultant forces allow for the trapping of the nanomaterials at the oil−water interface. As suggested in theory, these irregular-shaped particles produce a deformation of the fluid interface with undulated contact lines at the three phase contact line, which allow the trapping of particles at the oil−water interface.

CONCLUSION

By utilizing the concepts of fluid interface dynamics, a novel technique has been developed that can be utilized for separating nanomaterials from contaminated water. This methodology works quickly during processing and has nearly 100% efficiency. The extraction of functionalized nanomaterials is dependent on the concentration of surfactants used. If the concentration is sufficiently low, then the extraction is possible with high efficiency. Attempts to extract spherical particles confirmed that the shape of the particles has an effect on the extraction mechanism. Techniques for the extraction of spherical particles need even more investigation. The developed technique for separating 1D and 2D nanomaterials, such as nanotubes, nanosheets, and nanowires, from contaminated water allows for a simple and effective way to address the future environmental and health impacts of nanomaterials. The potential impacts of nanomaterials on environmental and health have gained significant attention as also highlighted in recent articles.[4−10,29−31]

ASSOCIATED CONTENT

Ⓢ Supporting Information

The Supporting Information is available free of charge on the ACS Publications website at DOI: 10.1021/acsami.5b07542.

Supporting figures (PDF)

AUTHOR INFORMATION

Corresponding Author

*E-mail: ykyap@mtu.edu.

Present Address

‡Engineering Product Development, Singapore University of Technology and Design, 8 Somapah Road, Singapore 487372, Singapore.

Author Contributions

The manuscript was written through contributions of all authors. All authors have given approval to the final version of the manuscript. D.Y.Z. and Y.K.Y. made the hypothesis and designed the experiments; B.T., D.Y.Z., and B.H. fabricated the materials; B.T., D.Y.Z., C.H.L., and Y.K.Y. performed the experimental measurements; B.T., D.W., D.Y.Z., and Y.K.Y. analyzed the results and wrote the manuscript.

Notes

The authors declare no competing financial interest.

REFERENCES

(1) Zhang, L.; Webster, T. J. Nanotechnology and Nanomaterials: Promises for Improved Tissue Regeneration. *Nano Today* **2009**, *4*, 66−80.

(2) Islam, N.; Miyazaki, K. An Empirical Analysis of Nanotechnology Research Domains. *Technovation* **2010**, *30*, 229−237.

(3) Sharifi, S.; Behzadi, S.; Laurent, S.; Forrest, M. L.; Stroeve, P.; Mahmoudi, M. Toxicity of Nanomaterials. *Chem. Soc. Rev.* **2012**, *41*, 2323−2343.

(4) Scheringer, M. Nanoecotoxicology: Environmental Risks of Nanomaterials. *Nat. Nanotechnol.* **2008**, *3*, 322−323.

(5) Oberdörster, G.; Maynard, A.; Donaldson, K.; Castranova, V.; Fitzpatrick, J.; Ausman, K.; Carter, J.; Karn, B.; Kreyling, W.; Lai, D.; et al. Principles for Characterizing the Potential Human Health Effects from Exposure to Nanomaterials: Elements of A Screening Strategy. *Part. Fibre Toxicol.* **2005**, *2*, 8.

(6) Behra, R.; Krug, H. Nanoparticles at Large. *Nat. Nanotechnol.* **2008**, *3*, 253−254.

(7) Balas, F.; Arruebo, M.; Urrutia, J.; Santamaria, J. Reported Nanosafety Practices in Research Laboratories Worldwide. *Nat. Nanotechnol.* **2010**, *5*, 93−96.

(8) Foss Hansen, S.; Maynard, A.; Baun, A.; Tickner, J. A. Late Lessons from Early Warnings for Nanotechnology. *Nat. Nanotechnol.* **2008**, *3*, 444−447.

(9) Morris, J.; Willis, J.; De Martinis, D.; Hansen, B.; Laursen, H.; Sintes, J. R.; Kearns, P.; Gonzalez, M. Science Policy Considerations for Responsible Nanotechnology Decisions. *Nat. Nanotechnol.* **2011**, *6*, 73−77.

(10) Linkov, I.; Bates, M. E.; Canis, L. J.; Seager, T. P.; Keisler, J. M. A Decision-Directed Approach for Prioritizing Research into The Impact of Nanomaterials on The Environment and Human Health. *Nat. Nanotechnol.* **2011**, *6*, 784−787.

(11) Tiwari, B.; Zhang, D. Y.; Yap, Y. K. *Efficient Extraction of Nanomaterials from Water Contaminated with Various Nanotubes, Nanosheets, and Nanoparticles.* 2014 Materials Research Society Spring Meeting, San Francisco, CA, April 21−25, 2014, Paper MM 10.04.

(12) Kayastha, V.; Yap, Y. K.; Dimovski, S.; Gogotsi, Y. Controlling Dissociative Adsorption for Effective Growth of Carbon Nanotubes. *Appl. Phys. Lett.* **2004**, *85*, 3265−3267.

(13) Kayastha, V. K.; Yap, Y. K.; Pan, Z.; Ivanov, I. N.; Puretzky, A. A.; Geohegan, D. B. High-density vertically aligned multiwalled carbon nanotubes with tubular structures. *Appl. Phys. Lett.* **2005**, *86*, 253105.

(14) Lee, C. H.; Wang, J.; Kayatsha, V. K.; Huang, J. Y.; Yap, Y. K. Effective Growth of Boron Nitride Nanotubes by Thermal Chemical Vapor Deposition. *Nanotechnology* **2008**, *19*, 455605.

(15) Lee, C. H.; Xie, M.; Kayastha, V.; Wang, J.; Yap, Y. K. Patterned Growth of Boron Nitride Nanotubes by Catalytic Chemical Vapor Deposition. *Chem. Mater.* **2010**, *22*, 1782−1787.

(16) Wang, J.; Lee, C. H.; Yap, Y. K. Recent Advancements in Boron Nitride Nanotubes. *Nanoscale* **2010**, *2*, 2028−2034.

(17) Mensah, S. L.; Kayastha, V. K.; Yap, Y. K. Selective Growth of Pure and Long ZnO Nanowires by Controlled Vapor Concentration Gradients. *J. Phys. Chem. C* **2007**, *111*, 16092−16095.

(18) Lee, C. H.; Zhang, D. Y.; Yap, Y. K. Functionalization, Dispersion, and Cutting of Boron Nitride Nanotubes in Water. *J. Phys. Chem. C* **2012**, *116*, 1798−1804.

(19) Velayudham, S.; Lee, C. H.; Xie, M.; Blair, D.; Bauman, N.; Yap, Y. K.; Green, A.; Liu, H. Noncovalent Functionalization of Boron Nitride Nanotubes with Poly(p-phenylene-ethynylene)s and Polythiophene. *ACS Appl. Mater. Interfaces* **2010**, *2*, 104−110.

(20) Ogino, K.; Onoe, Y.; Abe, M.; Ono, H.; Bessho, K. Reduced of Surface Tension by Novel Polymer Surfactants. *Langmuir* **1990**, *6*, 1330.

(21) Kralchevsky, P.; Paunov, V.; Ivanov, I.; Nagayama, K. Capillary Meniscus Interaction Between Colloidal Particles Attached to A Liquid—Fluid Interface. *J. Colloid Interface Sci.* **1992**, *151*, 79—94.

(22) Cavallaro, M.; Botto, L.; Lewandowski, E. P.; Wang, M.; Stebe, K. J. Curvature-Driven Capillary Migration and Assembly of Rod-Like Particles. *Proc. Natl. Acad. Sci. U. S. A.* **2011**, *108*, 20923—20928.

(23) Binks, B. P.; Horozov, T. S. Colloidal Particles at Liquid Interfaces: An Introduction. In *Colloidal Particles at Liquid Interfaces*; Binks, B. P., Horozov, T. S., Eds.; Cambridge University Press: Cambridge, 2006; pp 1—74.

(24) Lee, C. H.; Zhang, D. Y.; Yap, Y. K. Functionalization, Dispersion, and Cutting of Boron Nitride Nanotubes in Water. *J. Phys. Chem. C* **2012**, *116*, 1798—1804.

(25) Furst, E. M. Directing Colloidal Assembly at Fluid Interfaces. *Proc. Natl. Acad. Sci. U. S. A.* **2011**, *108*, 20853—20854.

(26) Oettel, M.; Dietrich, S. Colloidal Interactions at Fluid Interfaces. *Langmuir* **2008**, *24*, 1425—1441.

(27) Danov, K. D.; Kralchevsky, P. A. Capillary Forces Between Particles at A Liquid Interface: General Theoretical Approach and Interactions Between Capillary Multipoles. *Adv. Colloid Interface Sci.* **2010**, *154*, 91—103.

(28) Lewandowski, E. P.; Cavallaro, M., Jr; Botto, L.; Bernate, J. C.; Garbin, V.; Stebe, K. J. Orientation and Self-Assembly of Cylindrical Particles by Anisotropic Capillary Interactions. *Langmuir* **2010**, *26*, 15142—15154.

(29) Malysheva, A.; Lombi, E.; Voelcker, H. Bridging the Devide between Human and Environmental Nanotoxicology. *Nat. Nanotechnol.* **2015**, *10*, 835—844.

(30) Montaño, M. D.; Lowry, G. V.; von der Kammer, F.; Blue, J.; Ranville, J. F. Current Status and Future Direction for Examining Engineered Nanoparticles in Natural Systems. *Environ. Chem.* **2014**, *11*, 351—366.

(31) Meesters, J. A.; Veltman, K.; Hendriks, A. J.; van de Meent, D. Environmental Exposure Assessment of Engineered Nanoparticles: Why REACH Needs Adjustment. *Integr. Environ. Assess. Manage.* **2013**, *9*, e15—e26.

Supporting Information

A Simple and Universal Technique to Extract One- and Two- Dimensional Nanomaterials from Contaminated Water

Bishnu Tiwari,[1] Dongyan Zhang,[1] Dustin Winslow,[1] Chee Huei Lee,[1,2] Boyi Hao,[1]

Yoke Khin Yap[1,]*

[1]Department of Physics, Michigan Technological University, 1400 Townsend Drive, Houghton, MI 49931, USA. [2] Now at Engineering Product Development, Singapore University of Technology and Design, 8 Somapah Road, Singapore 487372

* To whom correspondence should be addressed. E-mail: ykyap@mtu.edu
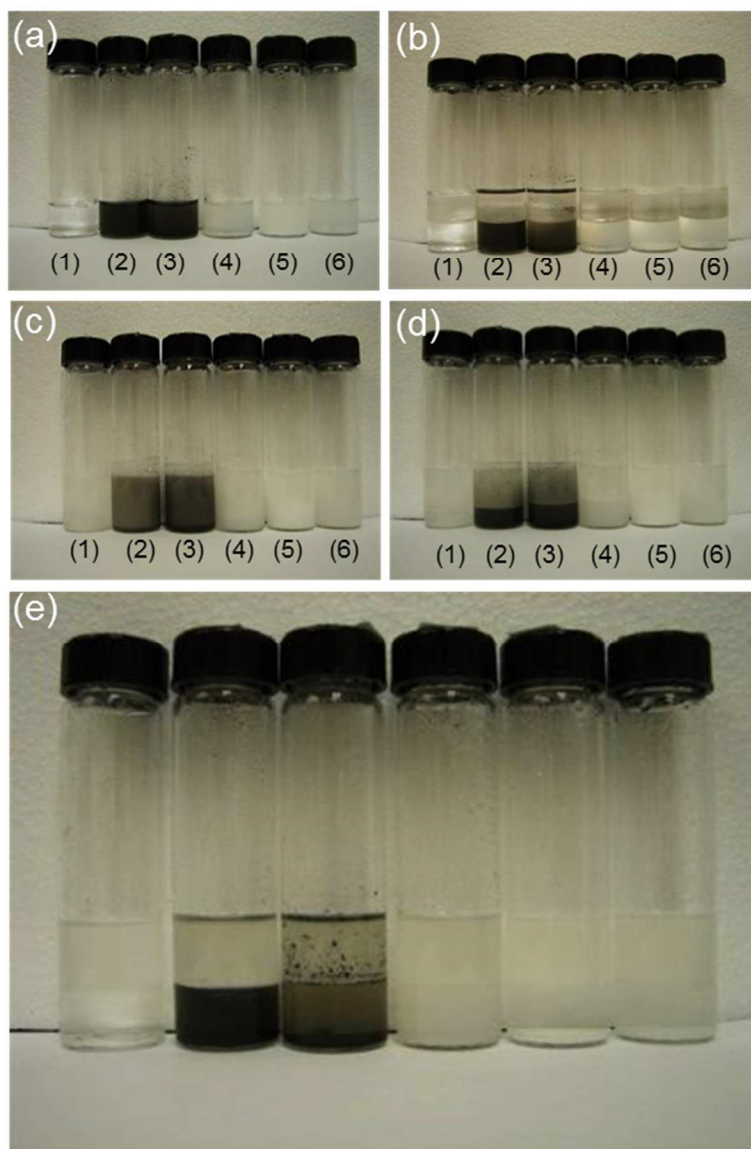
Figure S1. From left to right bottle in each picture are 1) distilled water, 2) MWCNTs in sodium cholate (SC) solution, 3) graphene in SC solution, 4) BNNTs in SC solution, 5) BNNSs in SC solution, 6) ZnO NWs in SC solution. (a) As suspended samples, (b) after adding oil on top, (c) after forming emulsion by handshaking, (d) 2 minutes after emulsification, (e) 1 day after emulsification.
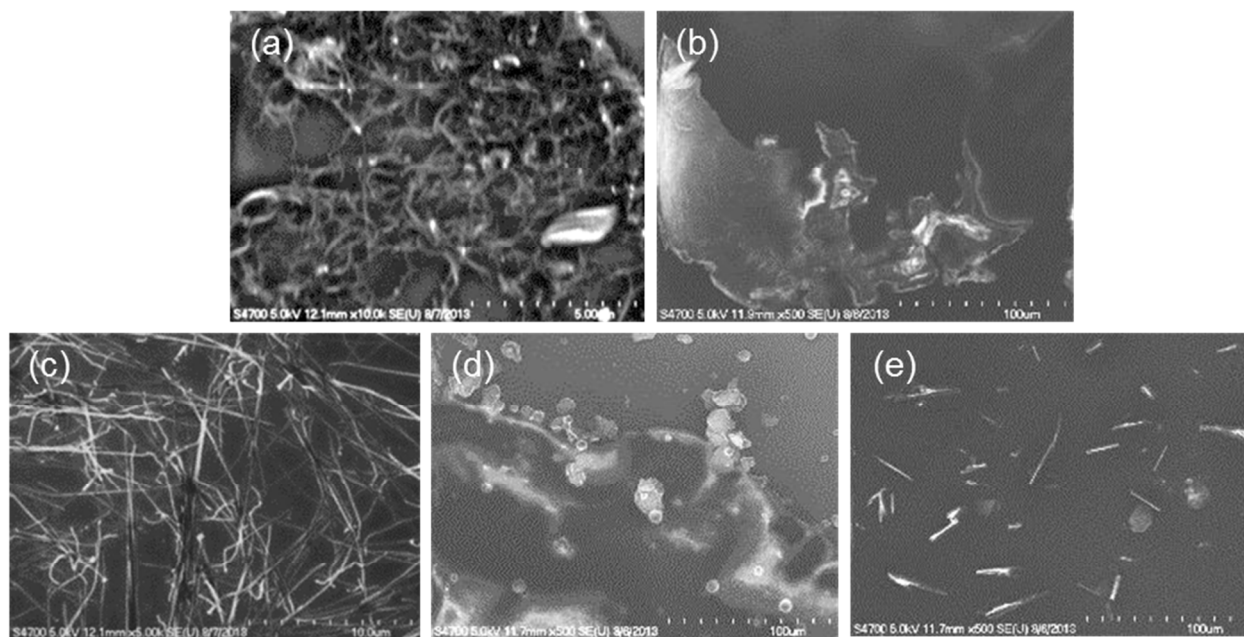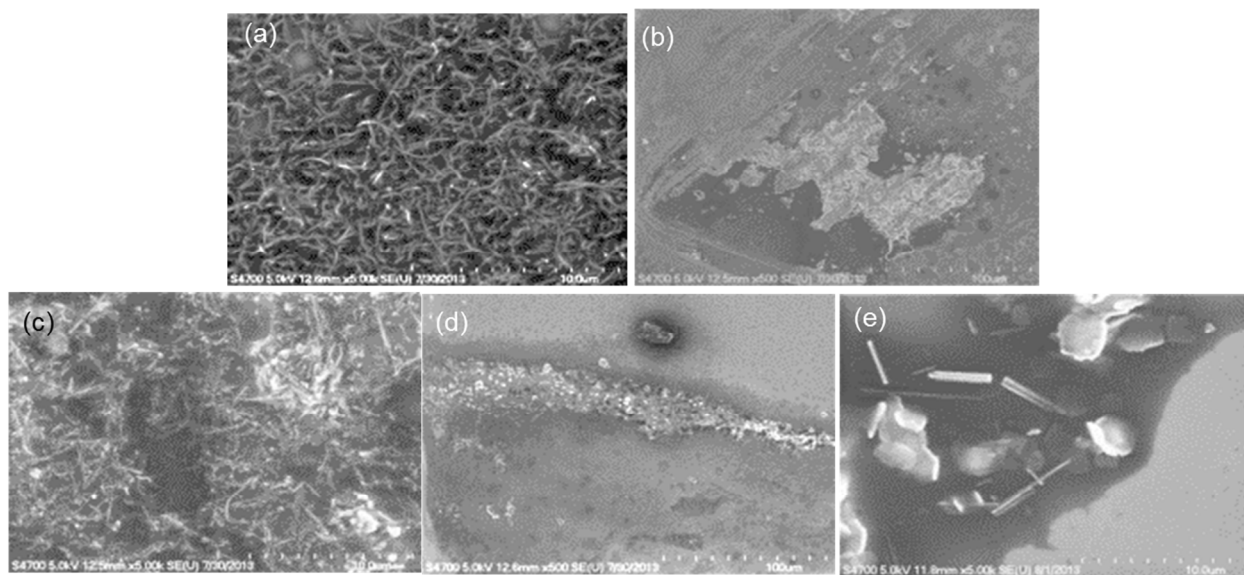
Figure S2. FESEM images of (a) MWCNTs (b) graphene (c) BNNTs (d) BNNSs and (e) ZnO

NWs sampled from the water phase (sodium cholate solution) after the extraction process.
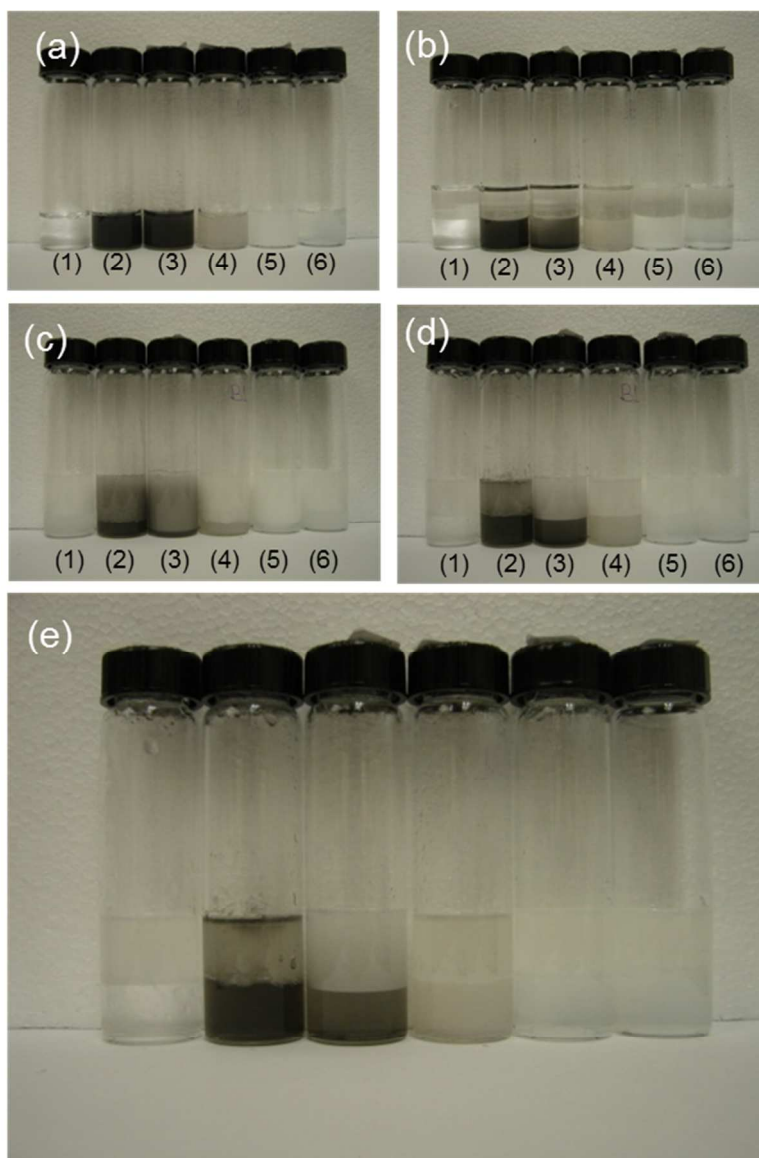
Figure S3. From left to right bottle in each picture are 1) distilled water, 2) MWCNTs in mPEG-DSPE solution, 3) graphene in mPEG-DSPE solution, 4) BNNTs in mPEG-DSPE solution, 5) BNNSs in mPEG-DSPE solution, 6) ZnO NWs in mPEG-DSPE solution. (a) As suspended samples, (b) after adding oil on top, (c) after forming emulsion by handshaking, (d) 2 hours after emulsification, (e) 1 day after emulsification.

Figure S4. FESEM images of (a) MWCNTs (b) graphene (c) BNNTs (d) BNNSs and (e) ZnO

NWs sampled from the water phase (mPEG-DSPE solution) after the extraction process.
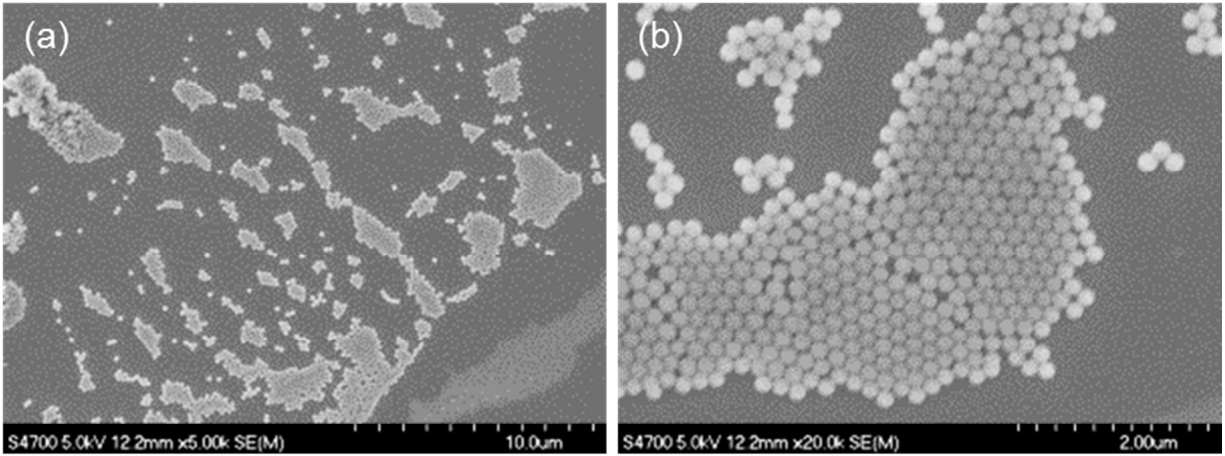
Silica sphere before processing
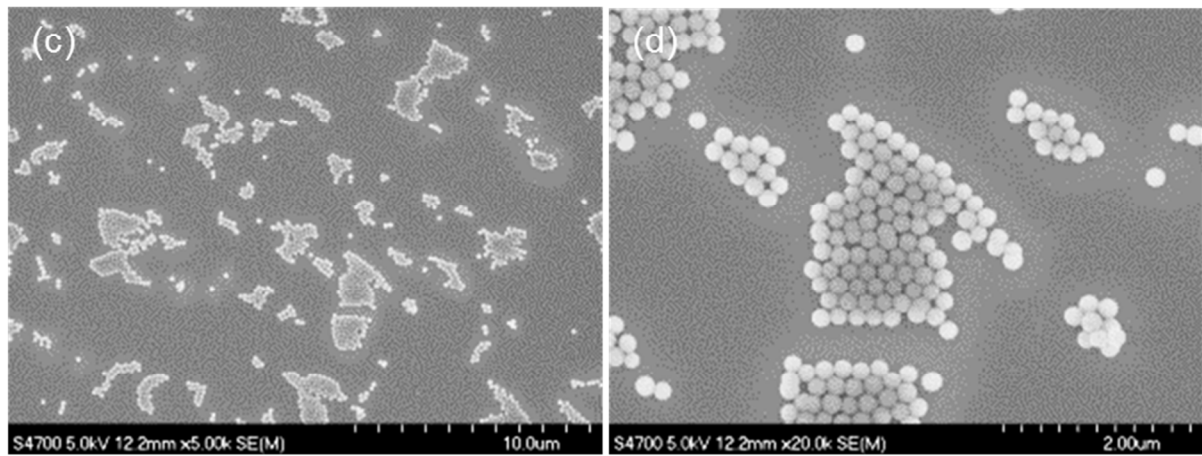
Silica sphere after processing

Figure S5. FESEM images of silica nanospheres samples collected a) and b) before extraction, and c) and d) after extraction.
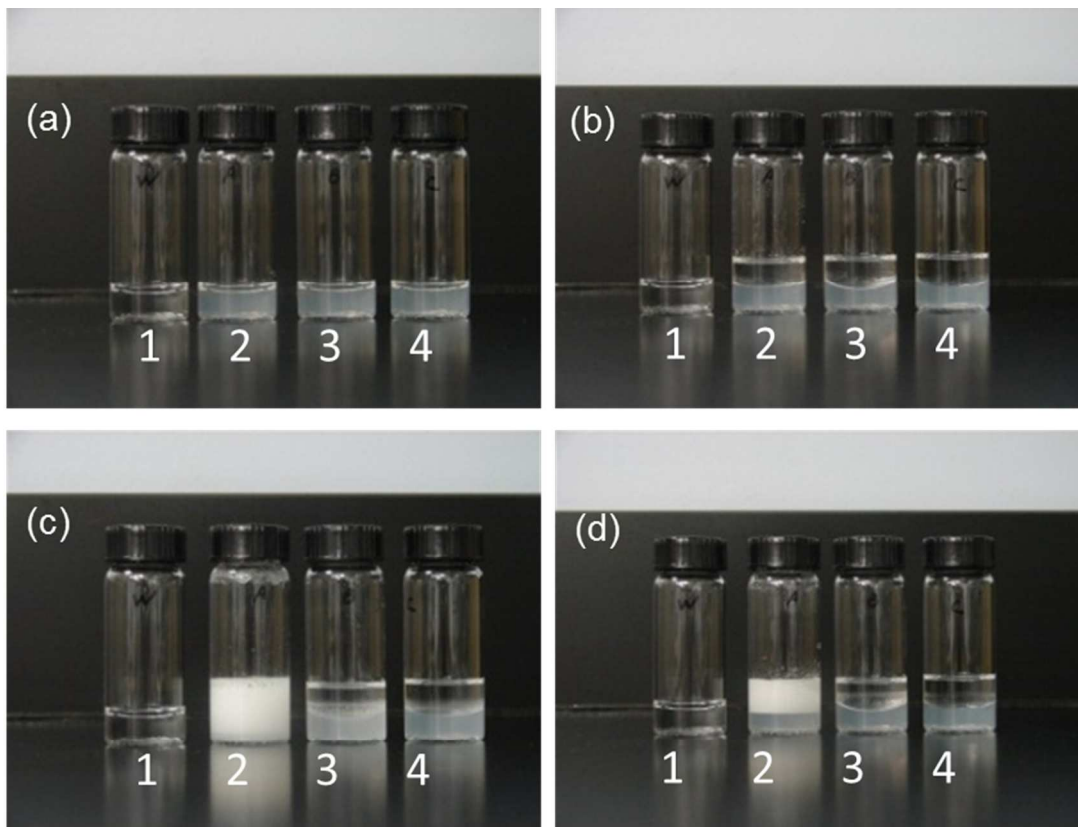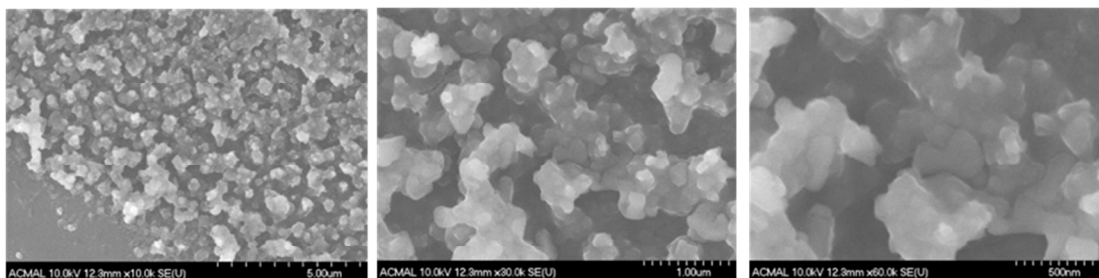
Figure S6. (a) As prepared sample with distilled water (1) and three suspensions of polystyrene spheres (2, 3, 4). Samples b) after adding oil, toluene, and hexane in vial 2, 3, and 4, respectively. Samples (c) 2 hr, and (d) 1 day after emulsification by handshaking.

FESEM images of sample from toluene phase after the extraction process:

FESEM images of sample from hexane phase after the extraction process:
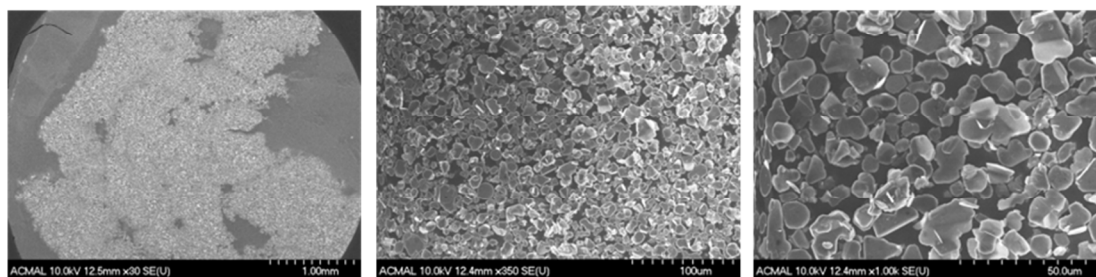

Figure S7. FESEM images of BNNSs in the toluene (top row) and hexane (bottom row) after the extraction.